ISTITUTO NAZIONALE DI FISICA NUCLEARE

Sezione di Milano

A polarizability model of the emission
from ceramic cathodes

Ilario Boscolo and Simone Cialdi
INFN-Sezione di Milano, Dip. di Fisica, Univ. di Milano, I-20133, Italy

Abstract

We show that properly electroded ceramic disks are strong and robust electron emitters when excited with short voltage pulses. We present in the article a phenomenological view of the processes which is capable of explaining all the experimental observations.

PACS:41.75.i, 41.85.Ar,77.80.e, 84.70+p

1   Introduction

Ferroelectric cathodes can operate in two different regimes: (I) a regime at low exciting voltage, $\sim 0.7\ kV$ per millimeter thickness and (II) a regime at high exciting voltage, $\sim 2\ kV/mm$. In the first regime the excitation pulse must be bipolar, positive-negative, the output current results in several tens of milli-amperes per cm^2. The first positive semi-wave charges the cathode surface and the negative semi-wave expels the previously accumulated electrons. This behavior of ceramic electroded disks, before as sink and next as source of electrons, is due to the succession of an attractive and then repulsive electron field on the un-electroded zones of the front surface. The two opposite oriented fields are generated by the voltage applied at the rear electrode. In the second regime, the excitation pulse can be either monopolar or bipolar, the emission process is governed by the building up of a plasma sheet as consequence of the excitation pulse. The high voltage exciting pulse initiates a discharge, and so a plasma, at the triple metal-insulator-vacuum point because of a strong longitudinal component of the electric field. The plasma cloud expands over the front surface becoming a dynamical electrode. Screening electrons accumulate in front of the sample, either in the plasma sheet or on the front surface of the material. The component of the electric field perpendicular to the surface (due to either the negative semi-wave of a bipolar pulse or to the space charge of the huge amount of electrons not anymore attracted by bound positive charge) pushes screening electrons out from the cathode.

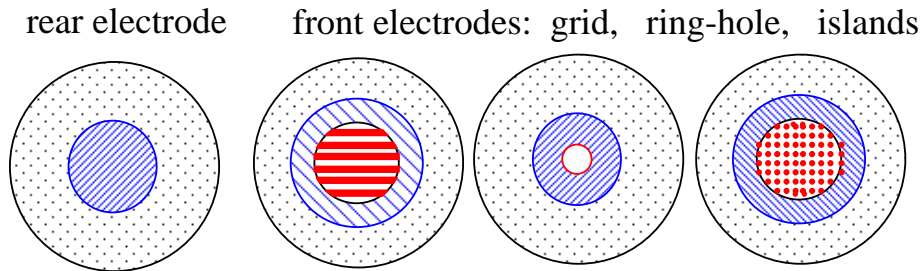rear electrode   front electrodes: grid, ring-hole, islands

Figure 1: Sketch of the cathode with different front electrodes used in the experiments of the article.

A typical ferroelectric cathode is a ceramic disk of high dielectric constant ϵ (1000 is a number to refer to) with a metallic film on the rear surface and a $400\ \mu m$ period grid ($200\ \mu m$ metalized and $200\ \mu m$ bare strips) interconnected by an external ring on the front surface [1–10], see Fig.1. A different front electrode pattern, a ring with inside a distribution of metallic patches (which we call *island electrode*) provided good features of these cathodes [11]. Electron emission occurs for the application at the rear electrode of an

2

exciting voltage pulse. In the several experiments reported in literature, the voltage pulse is required to be fast rising (few nanoseconds), a couple of kV per millimeter thickness and either negative or positive or bipolar. Strong emission was explained by nanosecond switching of ferroelectric domains or fast antiferroelectric-ferroelectric phase transition induced by a fast rising electric field on ceramics having a specific composition [1–6]. This view does not explain the emission from ceramics in paraelectric phase [12,13] and the different behavior between the cathodes with grid and with island electrodes [11]. The aim of this article is to give a contribution to the knowledge of the nature of the emission process, investigating in detail both the electron flowing in and the electron escaping from the cathode.

We have addressed our investigation separately on the charging and on the emission processes on materials in ferroelectric and paraelectric phases. We have found that both processes depend on the physical phenomena occurring at the metal-material-vacuum triple point at the application of the exciting voltage pulse and on the value of the dielectric constant ϵ. The geometry of the front electrode pattern defines the electric field distribution on the surface, hence it is important in determining the behavior of the cathode. We could not single out specific effects of the spontaneous polarization P_s.
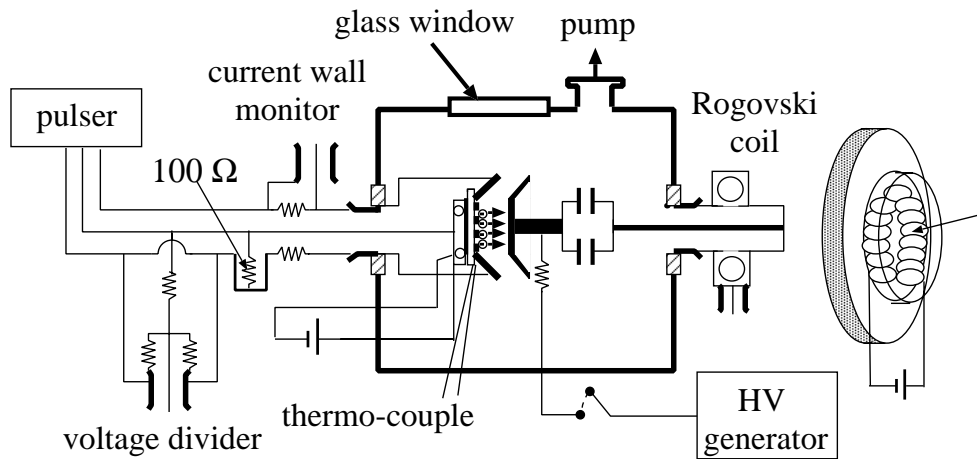

Figure 2: Sketch of the setup for voltage, displacement and emission current measurements; the displacement current is measured by a wall-current-monitor and the emission current by a Rogowski coil, a voltage divider measures the voltage pulse. The cathode is inserted in a Pierce designed diode. The HV-generator is connected or not depending on the kind of measurement is wanted.

We address mostly our attention to the emission without the application of an accelerating voltage through the diode gap with an external high voltage generator, see Fig. 2. These ceramic cathodes have the feature of emitting energetic electrons for the action

of the exciting pulse applied at the rear electrode. This peculiar feature of providing energetic electrons without the need of an electron gun structure in front of the cathode, allowed the implementation of a ceramic cathode in an ion source with a succesfull enhancement of its yield. [14,15].

We present the features, as source of electrons, of the different experimental configurations: different shapes of the front electrode, different waveforms of the excitation pulse, different materials and finally with and without a controlling mesh in the front of the cathode.

2   The physics of the emission

In this article, we show that the electrons are emitted from the metal border of the front grounded electrode at the application of a positive voltage pulse at the rear electrode. The emission is governed by the Fowler-Nordheim law as long as the voltage does not overcome the level of micro-discharge (and hence of plasma) ignition. In the Fowler-Nordheim regime electrons are attracted on the front surface when a positive voltage is applied at the rear electrode. This because an attractive field sets on the face. These deposited electrons are pushed out from the surface reversing the rear electrode voltage, thus reversing the front field. Hence, a bipolar high voltage exciting pulse does both electron extraction and expulsion from the surface. This conclusion is supported by the field configuration computed with Poisson program for the cathode with the ring-hole front electrode, see Fig. 1. When the exciting pulse is high enough, a plasma is initiated at the metal-material-vacuum triple point [5,16,17] and, because of it, the emission becomes strong. In this second case, the bipolar pulse is not needed: with a positive pulse, the amount of charge required for screening the induced polarization of the sample is so high that, when the pulse is over, the space charge force results enough strong to launch electrons from the cathode. The yield is obviously increased applying a negative pulse.

For our investigations, we have considered cathodes with ring-hole electrode so to have cylindrical geometry. This symmetry allows the calculations of the field configuration with the Poisson computer program.

Fig. 3 shows the result: the larger the internal diameter of the ring the higher the tangential field intensity is at the metal border. In addition, the figure shows that the voltage at the surface center increases with the enlargement of the hole. The increase of the field and the voltage with the enlargement of the internal radius has obviously a saturation. At that point, the electric field results mostly tangential to the surface at the border and the voltage at the center assumes the value of the rear electrode. We note that the same evolution of the field configuration occurs with the increase of the
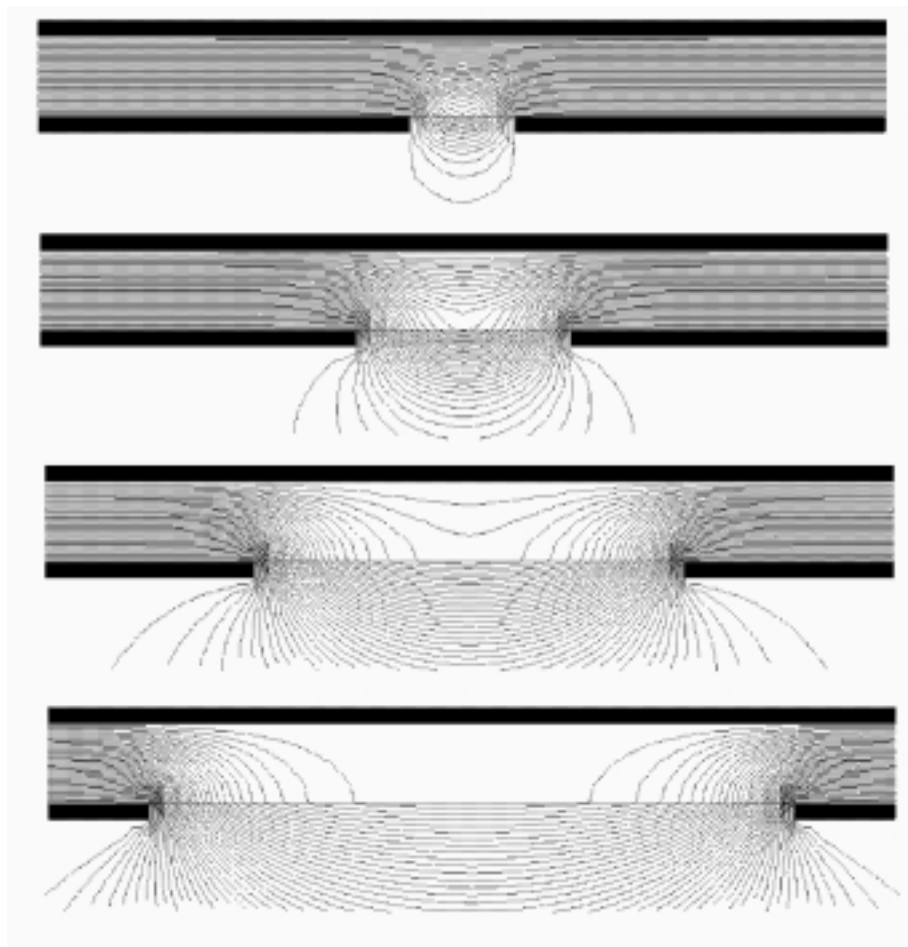
Figure 3: Electric field map obtained with Poisson computer program for the ring-hole front electrode: the succession refers to 1-2-4-6 mm respectively. The enhancement of the surface tangential field with the increase of the ring internal diameter is evident.

strip interdistance of a grid [18]. We believe that the high level of the exciting pulse, 4-5 kV/mm, required for observing emission with the grid electrode is due to the field segregation under the metallic strips. Incidentally, this voltage level is near to the sample damage limit.

When the tangential field is so high that a plasma sheet is formed [5,16,19], the plasma expands and connects electrically the whole surface. This plasma plays the role of an electrode: it allows the full polarization of the disk and it provides, in turn, the screening charges to the front surface.

Our picture of the emission process does not require the switching of the spontaneous polarization P_s. In fact, we show also that electron emission occurs with antiferroelectric, ferroelectric and paraelectric materials. In our experiments we have seen that the

important characteristic of the material for the emission is a *high value of the dielectric constant ϵ*. We could not see a clear action of the spontaneous polarization switching in our experimental configurations. Because of this, we call our model *polarizability model*.

A comment about the switching of the spontaneous polarization P_s model is in order. In the switching model the excitation pulse is negative. The charging of screening electrons on the un-electroded zones of the front surface is thought to be due to the plasma formation and expansion [5,17]. Here we present measurements in support of this view. The P_s variation under the un-electroded zones is driven by the plasma electrode. In the switching model, it is said that the spontaneous polarization P_s change occurs because of the high voltage pulse applied at the electrodes and it is not completely compensated by screening charge [20]. The un-compensated bound charge generates an electric field expelling screening electrons. This claim implies an efficient operation of the side-wall-motion mechanism [21] for the expansion of P_s from the electroded zones (where the field is segregated in the dense grid electrode owing to the high dielectric constant ϵ [22]) to the adjacent bare zones. We would like to point out that this mechanism operates only in a very neat conditions of both the surface and the bulk of the material [23,24]. In our operational conditions of a ceramic material with non-negligible glass and porous phases, of a surface contaminated owing to a dense plasma sheet formation at every exciting pulse, it is quite un-likely that the side-wall-motion mechanism can operate efficiently forth and back at each shot for many thousand shots. Along with this argument, we observe that the fringe field between the metallic strips has a component perpendicular to the surface. This field component acts upon electrons eventually set in front of the cathode because of the plasma and ejects them towards the anode.

Our picture of the emission explains the following observed results: a) the emission from ceramics in paraelectric phase [13,12] b) the poor emission from cathodes with very short period grid [11,4,25], c) the much better behavior of the island patterned cathodes [11,25] and d) the strong improvement of the emission with bipolar excitation [25]. Our new picture of the operation points out that the geometry of the front electrode and the dielectric constant of the material are the parameters to be considered: both must be chosen such as to have high tangential electric field at the border (for electron emission) and high perpendicular field (for electron ejection).

3 Charging of the cathode

The emission process has two phases in succession: I) the electron charging on the bare zones of the front surface and II) the appearing of a force which launches a fraction of the accumulated (screening) electrons from the surface towards the cathode. We try to

6

analyze separately the two processes.

3.1   The experimental set-up

The sketch of the apparatus used for the measurements is shown in Fig. 2. The cathodes with the three kinds of front electrodes are shown in Fig. 1. For our tests we have used mostly ring-hole electroded cathodes, because of easy technology, but also, more important, of easy field pattern computation. Our cathodes had one millimeter thickness. The anode cathode gap is about 20 mm. We have done the set of tests with many kinds of material: lanthanum doped (8%) lead (92%) titanate (65%) zirconate (35%), denominated PLZT 8/65/35, lead (71%) barium (29%) zirconate (70%) titanate (30%), denominated PBZT, lanthanum doped doped (4%) lead (96%) titanate (95%) zirconate (5%), denominated PLZT 4/95/5 and, finally, $SrTiO_3$, ceramics. The first two materials are in ferroelectric phase at room temperature, the third material is in antiferroelectric phase, while the last material is in paraelectric phase (it is in ferroelectric phase at less than $40\ K$). These materials gave scientifically consistent results. We report here only the results obtained with PLZT 8/65/35; they are typical for all the tested ceramics. The sample is heated by a light source located just behind the sample. The light source is a wrapped resistive nickel wire fed by a current as a light bulb, see detail in Fig. 2. A thermocouple, glued at the border of the disk, measures the sample temperature. A high voltage generator can be connected and disconnected from the anode, see detail in Fig. 2, so to apply or not an external accelerating voltage through the diode gap. When no external accelerating voltage is applied through the gap, only the electrons acted upon by a repulsive force created at the surface are collected. The $0.3\ \mu F$ capacitor inserted behind the anode, decouples it from ground for the application of the external voltage V_{acc}. That decoupling capacitor behaves as a short circuit for the short current pulses, thanks to the high value of its capacitance.

3.2   The surface charging

We start considering the cathode with the typical grid electrode. Screening electrons must be conveyed onto the un-electroded zones via the front grounded metallic strips. Electron migration from the rear electrode is very poor because of the high resistivity of the material. The electron flux from the metallic strips towards the neighboring non-metalized zones may occur, in principle, either through the material surface or through the vacuum (just over the surface) when the exciting voltage pulse is applied. Considering the high resistivity of the material and the strong enhancement of the electric field at the metal-material- vacuum triple point (because of the high value of the material dielectric
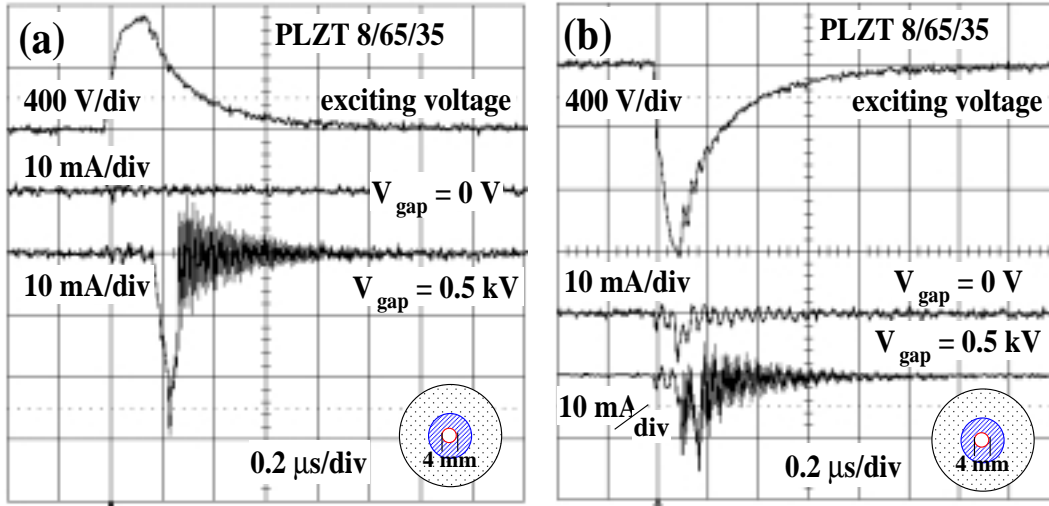
7

Figure 4: Excitation pulse, upper trace and current waveforms, the other two traces, with a cathode having as front electrode only a ring with 4 mm internal diameter, see previous figure. The mid trace is obtained with zero accelerating voltage through the diode gap, while the lower current trace is obtained with 0.5 kV accelerating voltage applied through the diode gap. The current recorded when the accelerating voltage is applied means that electrons are emitted in vacuum from the borders. They are all collected by the un-electroded internal area when no external filed is applied, as shown by the zero current mid trace. Charge is collected at the anode when a bipolar pulse is applied, frame (b). No emission is observed when a negative pulse is applied without a previous positive pulse.

constant), we may argue that the electron flux occurs through vacuum. The segregation of the field under the metallic strips does not allow the reduction of the surface resistivity reported in strongly polarized samples [26].

Our arguments are supported by the results of Figs. 4 and 5. Frame (a) of Fig. 4 shows that a current pulse is measured when a positive excitation pulse V_{exc} is applied to the sample and an accelerating voltage V_{acc} is applied through the diode gap. Hence, electrons are emitted at the cathode surface. Without V_{acc} no current is measured, the emitted charge is attracted by the un-electroded area of the surface, where the electrons stick on. Frame (b) of Fig. 4 shows that a current pulse is measured also without V_{acc} but with the application of a negative pulse at the rear electrode after a positive pulse application. No emission is observed with negative monopolar pulses of that amplitude: a previous positive pulse is needed for setting electrons on the surface. The negative pulse of Fig. 4 was applied many seconds after the positive pulse. The exciting pulse height for obtaining emission decreases enlarging the hole diameter from 4 to 6 mm, see Fig. 5.

The emission from the border of the metallic strips is governed by the Fowler-
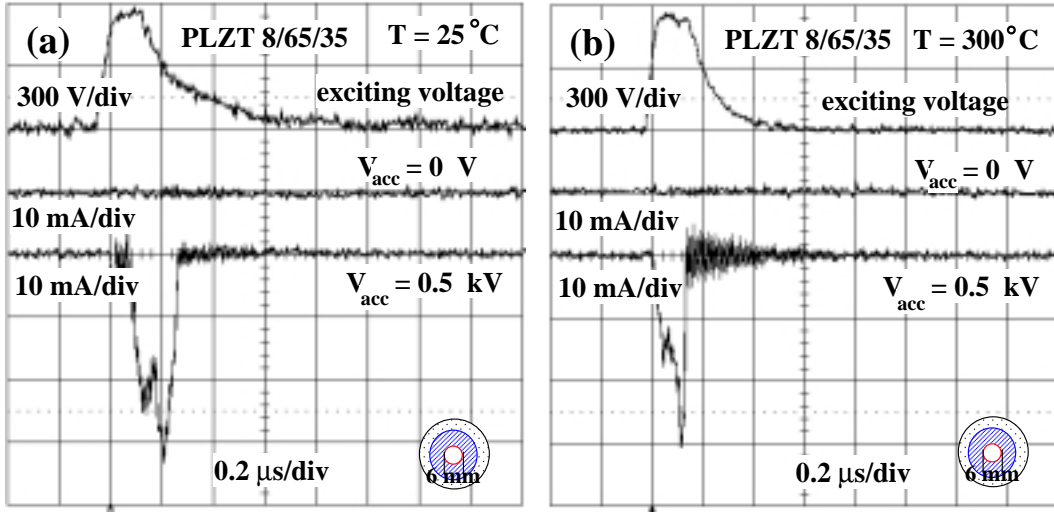
Figure 5: Excitation pulse, upper trace and current waveforms, the other two traces, with a cathode having the ring-hole of internal diameter of 6 mm as front electrode. The mid trace is obtained with zero accelerating voltage through the diode gap, while the lower current trace is obtained with 0.5 kV accelerating voltage applied through the diode gap. The emission begins at a voltage amplitude of 600 V, instead of the 750 V of the 4 mm case. Frame (b) shows the emission at $300\ ^oC$, where the sample is clearly in paraelectric phase: the two behaviors with sample in ferroelectric and in paraelectric phase are almost equal.
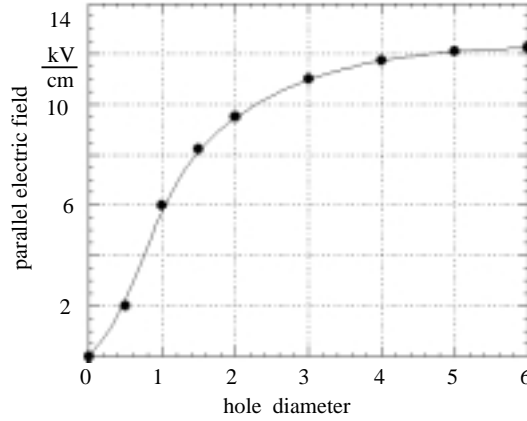

Figure 6: Diagram of the strength of the electric field component parallel to the sample surface at 0.2 mm distance from the border vs the radius of the internal circle of the ring-hole electrode. The calculations are referred to a pulse amplitude of 1 kV.

Nordheim law [6]. The field intensity can be estimated to have the value $E \sim (V_p \cdot \epsilon/\delta h) \cdot f(\phi)$, where V_p is the voltage amplitude of the applied pulse, δh is the sample thickness, ϕ is the diameter of the ring hole and $f(\phi)$ is a form function depending on the
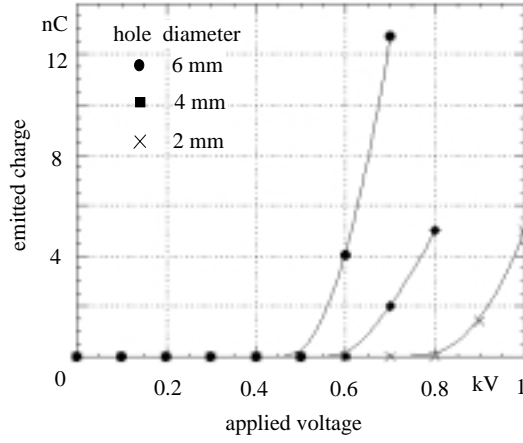
Figure 7: Diagram of the emitted charge vs the amplitude of the exciting voltage applied at the sample. The curve shows a threshold and afterwards its slope is very fast.

system geometry, as shown by the Fig. 6. The field increases very fast with the radius approaching the saturation value. From the Fowler-Nordheim law [27]

$$J = \frac{A}{\phi} \cdot (\beta E)^2 \cdot exp\left\{-\frac{B\,\phi^{3/2}}{\beta E}\right\} \tag{1}$$

we must expect a threshold value of the electric field strength for the field electron emission and then a fast slope as function of the field. This was, in fact, observed, as shown in Fig. 7, where the current vs the electric field applied at the sample is represented. In the above Eq. the quantities A and B hold the physics of a barrier tunneling and β is a phenomenological form factor introduced for matching the theory with experiments [28].

No light, neither faint, was seen in the charging and emission processes reported in previous figures. Because of this, this emission is called *dark emission* [4], contrary to the emission accompanied with the plasma formation, which is characterized by the presence of light .

3.3 The plasma ignition and the consequent behavior

When the exciting voltage is high enough, micro-discharges are initiated in some points of the metal border, see Fig. 8, and a surface plasma builds up. In order to check the action of the plasma as dynamical electrode, we have compared the charge fed to the sample as capacitor, see Fig. 9, with the polarization in a hysteresis cycle in sample with island electrode. The geometry of this electrode is suitable for this check because the area is mostly un-active without plasma and it becomes active with plasma. The charge absorbed by a sample covered by a plasma sheet was the same as measured in the hysteresis loop.
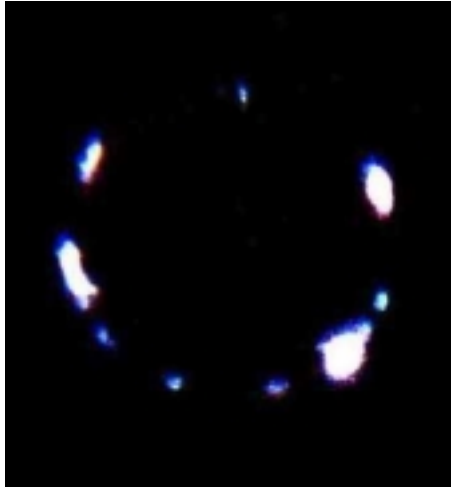
10

Figure 8: The figure shows the light emitted at the front surface of the cathode at the emission process.
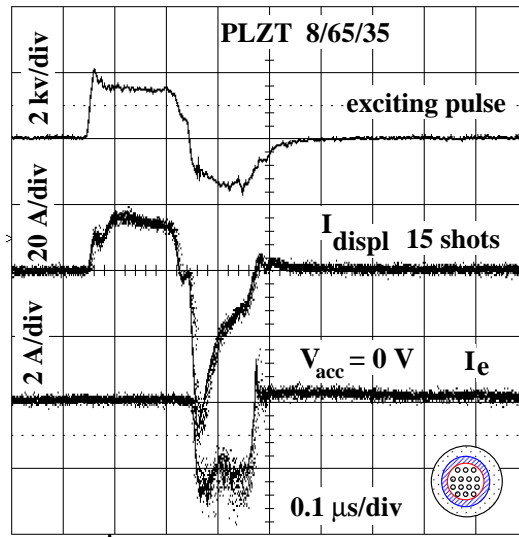

Figure 9: Typical signals obtained with PLZT 8/65/35 material: the upper trace is the exciting voltage pulse, the medium trace, I_{disp}, is the sample charging current and the bottom trace, I_e, is the emitted current. The non-symmetric shape of the positive side compared with the negative side of the displacement current I_{disp} is due to the fact that during the positive semi-wave a plasma sheet is building up and expanding over the sample surface, while at the negative semi-wave time the plasma covers the whole surface and behaves as an electrode.

It was, instead, the quantity relative to the metalized electrically connected area only, when the plasma did not form. We remark that in the measurement of Fig. 9 an island front electrode with a very thin ring was exploited because it permitted the best evidence
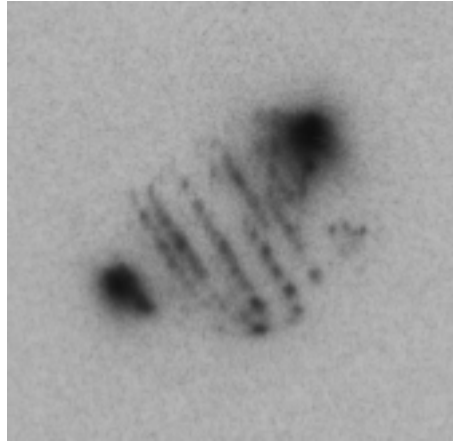
11

Figure 10: The figure shows the light emitted at the front surface of the cathode during the emission process. The diffuse light is a clear appearance of the plasma in front of the cathode.
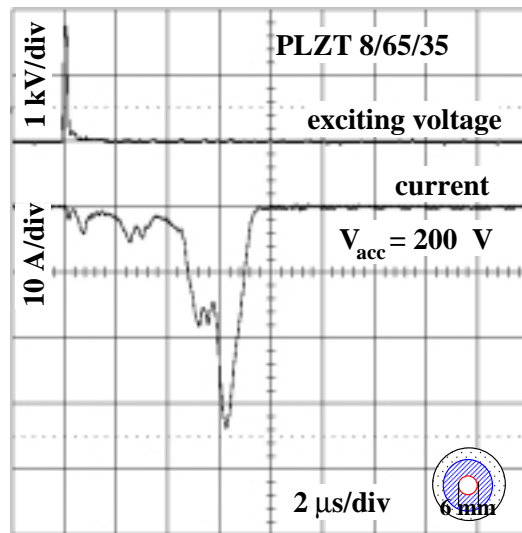

Figure 11: Emitted current when an accelerating voltage is applied at the cathode-anode diode. The current is much higher than without accelerating voltage, this is due to the plasma which fills up the diode gap: in this experimental configuration the whole charge of the buffer capacitor is within the area of the current signal.

of the plasma sheet action. Furthermore, a bipolar pulse was used, so to compare the displacement current shape during the first semi-wave, where the plasma is building up, with the behavior during the the subsequent semi-wave, where the plasma is already there. The displacement (charging) current of Fig. 9 shows, in fact, that in the first semi-wave the charging current is almost flat because the plasma is expanding over the surface, it has the typical shape of a capacitor charging in the second semi-wave.
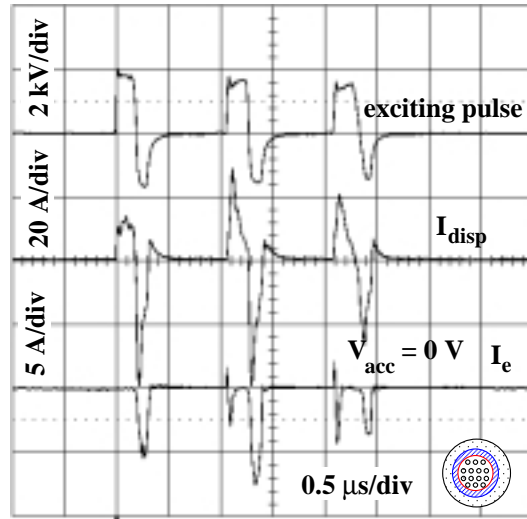
Figure 12: The emission, lower trace, at 1 MHz repetition frequency could be done with only three waves because the pulser did not have enough buffer charge to supply the sample capacitance for more than three shots, as shown by the decaying voltage amplitude of the exciting pulse, upper trace. The middle trace is the displacement current signal.
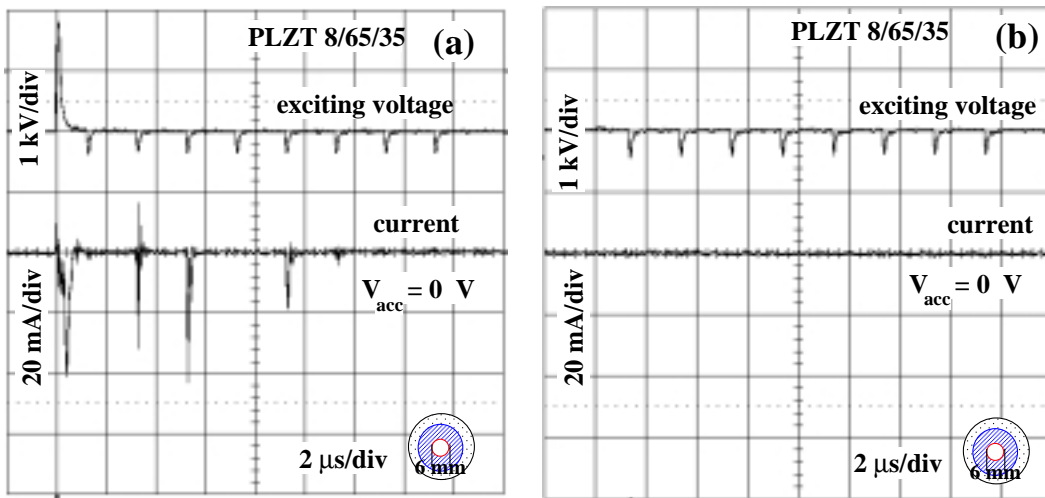

Figure 13: Frame (a) shows that a train of exciting negative pulses, whose amplitude is lower than that required for emission without the plasma, provides current during the duration time of the plasma within the diode. Frame (b) shows that no current is observed when the train of negative pulses is not preceded by a positive pulse excitation: this because the plasma is not built up.

The voltage amplitude required for the plasma ignition was around $2 \ kV/mm$. Figs. 10, 11, 12 and 13 show other four experimental evidences of plasma formation. The photo of the first figure shows the typical diffuse light of a plasma. The second figure

shows that the recorded current is much higher than the case without the accelerating field and, furthermore, its recording time is related to the time required by the plasma to close the diode gap. The diode impedance is almost zero, which says that the diode gap is filled of plasma. The third figure shows that the behavior of the sample complies with the presence of a virtual conductive sheet over the surface: the current pulses after the first are typical of a capacitor charging and discharging. The last measurement shows that when the plasma is set, frame (a) of Fig. 13, a train of *low* negative pulses can produce a correspondent train of current pulses as long as the plasma is alive. Frame (b) of that figure shows that without the positive pulse (that is without plasma) the train of current pulses is not produced.

The discharge initiation starts naturally from the metal borders when the exciting pulse is positive, being the metallic strips at negative potential with respect to the rear electrode and, therefore, with respect to the near bare zones. For the negative case, we must suppose an initial electron emission from atoms absorbed at the surface of the material and the melting of some points of the metal rim due to the impact with energetic electrons. The plasma ignition with negative excitation requires a pulse amplitude higher than that with positive excitation.

4   Electron emission

We must consider two different experimental configurations: (I) the configuration with an external accelerating field V_{acc} through the diode gap and (II) the configuration without an accelerating field through the diode gap. In this latter case we can single out the electrons launched from the surface with such an energy that they can overcome the counter force created by their own space charge.

4.1   Emission at low exciting voltage

We have to consider the two cases of positive pulse excitation and of negative pulse excitation.

Positive excitation pulse. Fig 4 shows in frame (a) the emission obtained with positive pulse excitation plus an accelerating voltage applied through the gap; frame (b) shows that emission occurs also without accelerating field, but with negative pulse excitation. The internal diameter of the ring-hole electrode was 4 mm. The emission without V_{acc} needs a previous surface charging (achieved applying a prior positive pulse at the rear electrode). The relatively low voltage applied in both cases assures that no plasma is initiated: we did not see either the discharge of the buffer capacitor through the diode gap or the typical lightning.

14

The measurements have been repeated with the front electrode ring having an internal diameter of 6 mm, see Fig. 5: the voltage threshold for observing the emission decreased. The relation between the threshold voltage for the emission, the internal diameter of the ring electrode, the Fowler-Nordheim law and the emission yield is not only internally very complex, but it is made further more complex by the screening effect of the charge deposited on the surface. Moreover, the samples are different one another whether for the material (it practically impossible to grow very equal materials) or for the electrode deposition. In addition, emission changes with the number of shots. Owing to all these out-of-control parameters, the trends shown by the figures repeated themselves in all other tests, the numbers did not.

With this 6 mm configuration, we have also investigated the emission at $300\ ^oC$ temperature, where the sample is clearly in paraelectric phase: Fig. 5 shows that the two emissions, at room temperature (where the sample is in ferroelectric phase) and that at high temperature (where the sample is in paraelectric phase) are substantially equal, as are the dielectric constants at the two temperatures. This results says that, if there is a contribution of the spontaneous polarization switching to the emission when the sample is in ferroelectric phase, it should not be important; the emission, in our experimental configuration, comes out to depend on the polarizability of the material [13].

Since the dark regime does not seem to have anything inconvenient against a high repetition rate operation, at least when samples are not in ferroelectric phase, we did a check and the result is shown in Fig. 14: samples in paraelectric phase operated neatly at high frequency.

On the base of the field amplitude vs the hole radius, coupled with Eq. 1, we have tested the emission with negative exciting pulse and $V_{acc} = 0$ with the 6 mm hole. The result is shown in Fig. 15. The pulse height is lower that that required by the 4 millimeter hole. Notice that the emission with an accelerating voltage applied between the cathode-anode is only a bit higher than that obtained without accelerating field. There is no trace of a plasma presence.

Negative excitation pulse. No emission is observed with negative excitation pulse only.

4.2   Emission at high exciting voltage

Fig. 16 shows the emission with positive excitation pulse and without accelerating field. The fact that the current signal shows up at the end of the pulse should suggest the following process: the positive voltage at the rear electrode leads to plasma formation (confirmed by previous measurements), the front plasma electrode together with the voltage
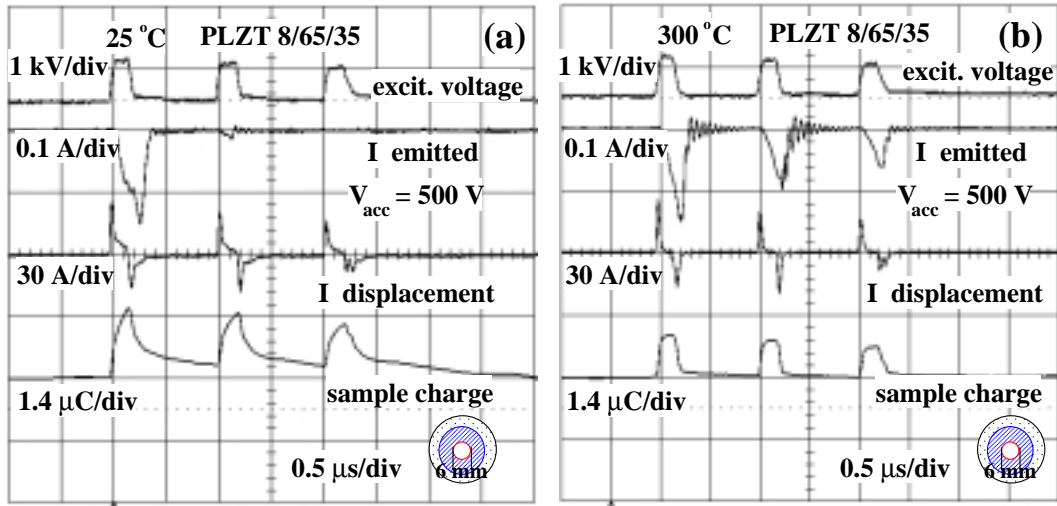
15

Figure 14: Succession of three pulses at 1 MHz in the dark regime: from the top, the first trace is the exciting voltage pulse, the second trace is the emitted current, the third trace is the displacement current and the forth trace is the integral of the displacement current, that is the charge on the sample. An accelerating voltage of 0.5 kV through the gap was applied. Notice the decrease of the pulse voltage, because of it we could not run our pulser with more than three shots. The sample was heated at $300\ ^oC$, hence it operated in paraelectric phase. Notice that at $25\ ^oC$ the relax time of the polarization is much longher than that at $300\ ^oC$.

of the rear electrode induce the sample polarization and in turn the accumulation of a huge amount of electrons on the front surface (because of the high ϵ), the polarization relaxes at the end of the pulse, see Fig. 14, and finally the sheet of electrons in excess on the sample surface creates an electric field repulsive for electrons set in front of the cathode. The emission of the sample in ferroelectric phase is not reproducible in amplitude and appearance, because it comes as consequence of the relaxation process of the spontaneous polarization. The above picture is experimentally supported by the large difference of the polarization relaxation time of samples in ferroelectric and paraelectric phase: the two frames of Fig. 14 show that the relaxation time of a sample in ferroelectric phase is in the micro-second scale, while it is in the nano-second scale in paraelectric phase. This difference leads to different emissions of the sample in the two thermodynamical phases, as shown by the two frames of the Fig. 16: frame (a) shows that a sample in ferroelectric phase gives an emission pulse of a couple hundred nanoseconds width and not reproducible, frame (b) shows that the same sample in paraelectric phase gives narrower, higher and substantially stable pulses. We point out that in the former case the polarization is mostly spontaneous polarization, whereas in the second case it is the normal polarization.
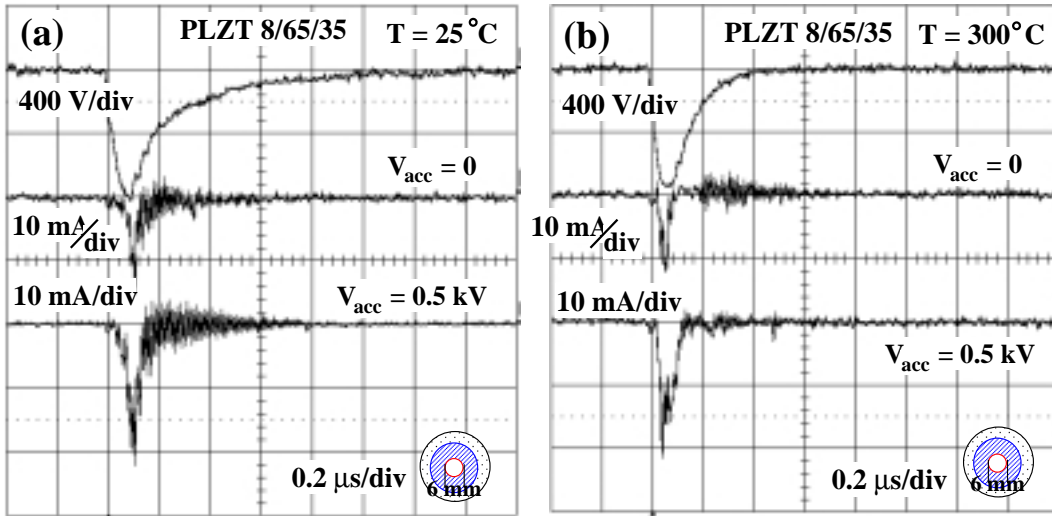
16

Figure 15: Emission observed with negative excitation pulse with and without an accelerating voltage set across the diode gap and after the application of a charging positive pulse. The current pulse with the accelerating field is only a bit higher than that without accelerating field. The long pulse typical when a plasma is formed does not show up, hence no plasma is formed.
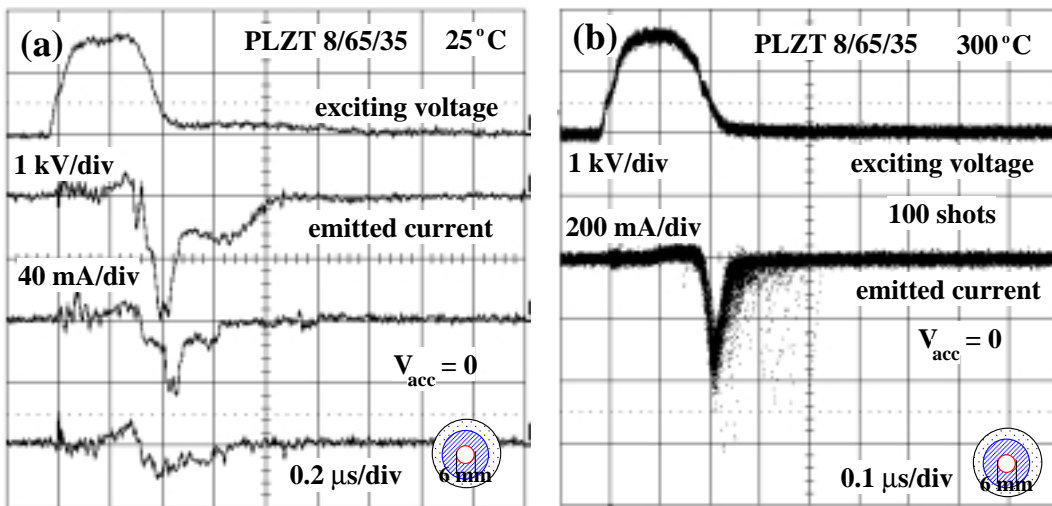

Figure 16: Current pulse obtained with positive exciting pulse of about 2 kV/mm and zero accelerating field at room and 300^oC, that is with the sample in ferroelectric and paraelectric phase. Frame (a) has three random shots for showing the emission instability. The behavior in paraelectric phase is better: higher current and stability.

We recall that Fig. 9 shows the result when a bipolar excitation pulse is applied and $V_{acc} = 0$ (with island electrode). The emitted current of energetic electrons is much higher when a negative pulse is put in succession to a positive exciting pulse. The emission

becomes also very stable [25].

We recall also that Fig.11 shows the emission with positive excitation and an external accelerating field. In this experimental conditions a plasma fills up the diode gap, hence the charge collected at the anode is $Q = VC$, that is the charge of the buffer capacitor, being C the capacitance of that capacitor and V its voltage (equal to the accelerating voltage). The group of the energetic electrons is the small peak just at the beginning of the trace.
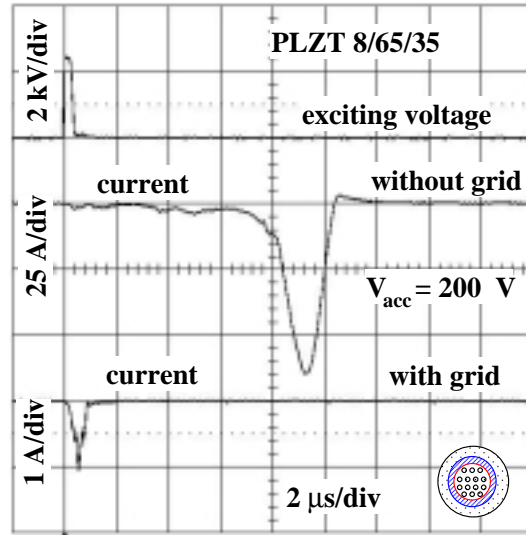

Figure 17: The center trace refers to the current obtained with $V_{acc} = 200\ V$ and without the screening mesh, the bottom trace is obtained in the same conditions of the above signal but with a screening mesh in front of the cathode. The high current signal is typical of the case of the diode gap filled by plasma. The lower signal indicates a clear screening action of the mesh.

The comment about this emission with the plasma formation is that this kind of emission can be useful in two experimental conditions: in the first, the diode gap is supplied by a short voltage pulse [29], in the second, a diaphragm transparent to electrons, keeps the plasma within a cathode area, so to prevent it from entering the accelerating section. In the first configuration, the plasma feeds electrons for the duration of the voltage pulse and does not have the time to propagate across the accelerating section during the presence of the pulse. For a test of the second configuration, we have put a screening mesh in front of the cathode, 5 mm ahead, kept at ground potential. In this configuration an external accelerating field cannot act on the plasma behind the mesh and the field lines from the sample surface (due to the exciting pulse) terminate on the mesh. Fig. 17 shows that a mesh does excellently the screening action: the diode gap is separated from the plasma produced in front of the cathode.
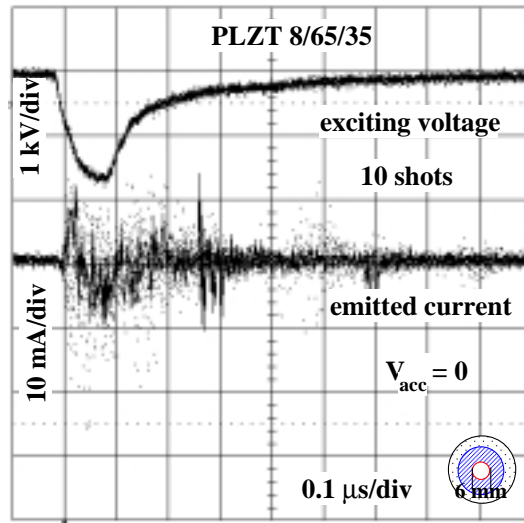
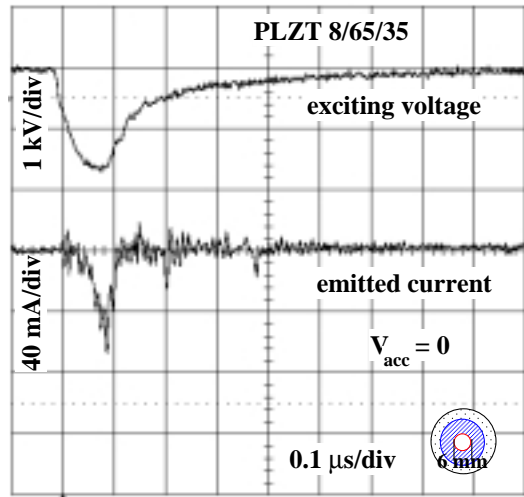Figure 18: Current pulse obtained with negative exciting pulse of about 2 kV/mm and zero accelerating field.

Figure 19: Current pulse obtained with negative exciting pulse of about 2 kV/mm and zero accelerating field, but after a positive pulse was applied.

Negative pulse. The cathode does not emit with monopolar negative excitation pulses, see Fig. 18, unless a previous positive (charging) pulse is applied, see Fig. 19. Emission, instead, occurs with monopolar negative pulses if the pulse amplitude is very high. The conjecture is that, while the plasma expands over the un-electroded zone, the repulsive field created on the surface by the negative exciting pulse expels electrons from the plasma cloud.

19

5 Conclusions

The investigation of the emission problem from high dielectric constant ceramic disks, through the two phases of the surface charging and successive electron expulsion, has shown to be very fruitful for understanding the physics of the problem. The main result of the investigation is that the voltage pulse needed for exciting the emission must be such that it can do the both jobs of before charging and then expelling electrons from the cathode. These two actions can be obtained managing a trade off among the pulse amplitude, pulse waveform, front electrode pattern and dielectric constant ϵ. Measurements have shown that good operations are obtained with samples in paraelectric phase, while samples in ferroelectric phase do not operate reliably. This un-reliable behavior is correlated with the relaxation of the spontaneous polarization.

Two operational regimes have been discovered: a *dark regime*, that is a regime without a plasma formation in front of the cathode, and a *plasma regime*, that is a regime with the plasma formation. The first regime operates at a critical voltage amplitude: this must be enough high to provide electron emission from the metallic border of the front electrode, but not so high to switch on micro-discharges. In this regime a paraelectric material has shown the capability to operate at high frequency, higher than 1 MHz. The current level is something about fifty milliamperes per cm^2. In the plasma regime, the current can be, obviously, very high. The characteristics of this kind of emission is that its timing can be controlled by the exciting pulse. The other important characteristic is that the cathode can supply a current of energetic electrons of many amperes per cm^2. The drawback is that the cathode area must be screened with diaphragms from the accelerating section.

The island electrode compared with the more common grid electrode has a much better performance because the tangential component of the electric at the metal border is greatly enhanced, as well as the voltage of the un-electroded zone increases. Hence, the charging and repulsive actions become efficient. The operations with bipolar positive-negative pulses are much better just because the two charging and repulsive actions are well defined.

At the end, we have demonstrated that the dielectric constant, that is the normal polarization, in conjunction with an electrode front design which allows the penetration of the electric field on the un-electroded zones of the surface, are the variables which decide the performance of the cathode. For this reason we have called our emission model *polarizability model*.

References

[1] H. Gundel, H. Riege, E.J.N. Wilson, J. Handerek and K. Zioutas, Nucl. Instrum. Meth. Phys. Res. A **280**, 1, 1989.

[2] H. Riege, Nuclear instruments and Methods in Phys. Res.A, **340**, 80, (1994).

[3] G. Rosenman and I. Rez, J. Appl. Phys. **73**, 1904, (1993).

[4] D. N. Shannon, P. W. Smith, P. J. Dobson, M. J. Shaw, Appl. Phys. Lett. **70**, 1625, (1997).

[5] G. Benedek, I. Boscolo, J. Handerek, H. Riege, J. Appl. Phys, **81**, 1396, (1997).

[6] D. Flechtner, C. Golkowski, J.D. Ivers, G.S. Kerslick, J.A. Nation, L. Schachner, J. Appl. Phys. **83**, 955, (1998).

[7] T.C. Cavazos, W.L. Wilbanks, C.B. Fleddermann, D.A. Shiffer, Appl. Phys. Lett. **65**, 2612, (1994).

[8] B. Jiang, G. Kirkman, N. Reinhardt, Appl. Phys. Lett. **66**, 1196, (1995).

[9] Weiming Zhang, wayne Huebner, J. Appl. Phys. **83**, 6064, (1998).

[10] F. liu, C.B. Fleddermann, Appl. Phys. lett. **76**, 1618, (2000)

[11] I. Boscolo, A. Scurati, M. Stellato, J. Appl. Phys, Vol. **85**, 8337-8342, (1999).

[12] M. Okuyama, J. Asano, Y. Hamakawa, Jpn., J. Appl. Phys. Part I **33**, 5507, (1994).

[13] I.Boscolo, S. Cialdi, Appl. Phys. Lett. **79**, 2001.

[14] I. Boscolo, S. Cialdi, G. Somare', M. Valentini, S. Gamino, G. Ciavola, L. Celona, S. Marletta, H. Riege, J. Handerek, EPAC2000 Conf. Wien June 2000.

[15] I.Boscolo, S. Cialdi, M. Valentini, S. Gammino, G. Ciavola, L. Celona, S. Marletta, H. Riege, J. Handerek, J. Appl. Phys. (to be pulblished)

[16] V. Puchkarev, A. Mesyats, J. Appl. Phys., **78**, 5633, (1995).

[17] Ya. E. Krasik, A. Dunaevsky, J. Felsteiner, J. Appl. Phys. **85**, 7946, (1999).

[18] L. Schachner, D. Flechtner, C. Golkowski, J.D. Ivers, J.A. Nation, J. Appl. Phys. **84**, 6528, (1998).

[19] A. Dunaevsky, Ya. E. Krasik, J. Felsteiner, S. Krokhmal, J. Appl. Phys. **87**, 3270, (2000).

[20] H. Riege, I. Boscolo, J. Handerek, U. Herleb, J. Appl. Phys. **84** ,1602, (1998).

[21] M. E. Lines and A.M. Glass, *Principles and Applications of Ferroelectric and Related Materials*, (Clarendon Press, Oxford, 1977).

[22] G. Benedek, I. Boscolo, J. Handerek, A. Moscatelli, A. Scurati, J. Appl. Phys, **83**, 2776, (1998).

[23] W. J. Merz , J. Appl. Phys. **77**, 938, (1956).

[24] R. C. Miller, A. Savage, Phys. Rev. **112**, 755, (1958)

[25] I.Boscolo, S.Cialdi, J. Appl. Phys. (to be published)

[26] W. Mock, Jr. and W. H. Holt J. Appl. Phys. **50**, 2740, (1979).

[27] R.H. Fowler and L. Nordheim, Proc. Roy. Soc. Lond., **A 119**, 173, (1928).

[28] H.A. Schwettman, J.P. Turneaure, R.F. Waites, J. Appl. Phys. **45**, 914, (1974).

[29] J.D. Ivers, D. Flechtner, C. Golkowski, G. Liu, J.A. Nation, L. Schachner, IEEE Trans. Plasma Science **27**, 707, (1999).